broid systematics because it provides a phylogenetic signal over an issue where morphology is equivocal due to homoplasy. In a maximum parsimony analysis of all informative nucleotide sites (*1*), billfishes composed one clade, and all other scombroids composed a separate clade. *Gasterochisma* was nested within the nonbillfish clade. In placing billfishes so distant from the scombrids, and thus the butterfly mackerel, our study provides strong evidence for two conclusions: cranial endothermy evolved two times, and it evolved independently in very distantly related lineages.

In 300 replications of the bootstrap procedure with the use of a heuristic search on all informative nucleotide sites (*5*), a grouping of all cranial endotherms (billfishes + *Gasterochisma*) did not occur. This finding (*3*) represents direct evidence against the monophyly of cranial endotherms (*6*). In a parsimony analysis of all informative amino acid sites (*7*), the strict consensus of 96 equally most parsimonious trees indicates separation of the billfish clade from *Gasterochisma*. Furthermore, a 10% increase in tree length is required to produce a topology that indicates monophyly of cranial endotherms (tree length increased from 111 to 122 amino acid substitutions). This difference in length represents highly significant statistical evidence against the monophyly of cranial endotherms according to the topology-dependent cladistic permutation test for nonmonophyly (*8*). Our phylogeny and that of Collette *et al.* (*3*) support the same conclusion about how many times these evolved but differ significantly from the morphological phylogeny of Johnson (*2*).

Beyond counting how many times endothermy has evolved we seek to understand the selective pressures that have favored the evolution of endothermy and the preadaptations that may have permitted its evolution in the Scombroidei. Thus, we must identify the ectothermic sister groups of the endothermic lineages.

The morphological hypotheses (*1*, *2*) consider billfishes to be derived scombroids that share a most recent common ancestry with members of the family Scombridae. *Gasterochisma* resides within the Scombridae in one of these studies (*2*). The molecular data (*3*) indicate that billfishes lie outside of a clade composed of all other scombroids, suggesting that cranial endothermy evolved independently in two very distant lineages. The morphological data of Collette *et al.* (*2*) suggest that cranial endothermy evolved twice within a group of closely related fishes: the clade composed of billfishes plus Scombridae.

We have recently completed a second molecular analysis on scombroid relationships based on the nuclear gene *lactate dehydrogenase b* (*9*). The *LDH b* nucleotide trees are similar to the *cytochrome b* trees and refute the monophyly of cranial endotherms with robust statistical support.

Johnson and Baldwin state that the addition of taxa could weaken the conclusions of our molecular phylogenetic analysis. This criticism could theoretically be leveled at any phylogenetic hypothesis. However, the addition (*10*) of taxa to the molecular phylogenetic analysis, including the wahoo, *Acanthocybium solandri*, a species which Johnson proposes is the sister group to billfishes, reinforces our conclusion (*3*) that the billfishes are distantly related to other scombroid fishes (Fig. 1). Furthermore, our analysis of this enlarged *cytochrome b* data set rejects the hypothesis by Johnson (*1*) that *Acanthocybium* is the sister-group of billfishes and is consistent with the placement of the wahoo made by Collette *et al.* (*2*). This conclusion is also strongly supported by the *LDH b* analysis.

Molecular data provide an important source of phylogenetic information for the Scombroidei, primarily because it complements existing morphological data and is informative in instances where morphological hypotheses conflict. We believe that historical patterns are best elucidated when a combination of different types of data, morphological and molecular, is used to corroborate and test phylogenetic hypotheses. We hope our study encourages such a synthesis.

John R. Finnerty
Barbara A. Block*
Department of Organismal Biology
and Anatomy, University of Chicago,
Chicago, IL 60637, USA

---

*Present address: Stanford University, Biological Sciences, Hopkins Marine Station, Pacific Grove, CA 93950, USA.

REFERENCES AND NOTES

1. G. D. Johnson, *Bull. Mar. Sci.* **39**, 1 (1986).
2. B. B. Collette, T. Potthoff, W. J. Richards, S. Ueyanagi, J. L. Russo, Y. Nishikawa, in *Ontogeny and Systematics of Fishes*, H. G. Moser *et al.*, Eds. (Spec. Publ. no. 1, Supplement to *Copeia*, American Society of Ichthyologists and Herpetologists, Lawrence, KS, 1984), pp. 591–620.
3. B. A. Block, J. R. Finnerty, A. F. R. Stewart, J. Kidd, *Science* **260**, 210 (1993).
4. T. Potthoff, S. Kelley, S. Ueyanagi, *Bull. Mar. Sci.* **30**, 329 (1980); I. Nakamura, *Publ. Seto Mar. Biol. Lab.* **28**, 255 (1983); T. Potthoff and S. Kelley, *Fish. Bull. U.S.* **84**, 647 (1986).
5. J. Felslenstein, *Evolution* **39**, 783 (1985).
6. In the same way that a high bootstrap value for a particular node indicates support for the monophyly of a group of taxonomic units, a low value represents evidence that a group of taxonomic units is not monophyletic (D. P. Faith, personal communication).
7. The *cytochrome b* nucleotide sequences used to construct the phylogeny in our report [figure 1 of (*1*)] were translated into amino acid sequences. A heuristic search for the most parsimonious tree was performed on these data with the use of *PAUP*, version 3.0s [Phylogenetic Analysis Using Parsimony, Swofford, D. L., 1990; tree-bissection and reconnection (TBR) branch swapping were performed on ten starting trees generated through random addition of taxa]. Ninety-six equally most parsimonious trees identified in the search indicated that *Gasterochisma* is nested within a clade containing members of the scombroid families Scombridae and Gempylidae and that billfishes fall outside of this clade. The "enforce topological constraints" option of PAUP was used to identify the most parsimonious topology that supported the monophyly of cranial endotherms, *Gasterochisma*, and billfishes. This topological constraint resulted in an 11-step increase in tree length over the most parsimonious tree (122 over 111 steps).
8. D. P. Faith, *Syst. Zool.* **27**, 401 (1991). We conducted topology-dependent cladistic permutation (T-PTP) tests for non-monophyly of cranial endotherms with the use of the inferred amino acid sequences from the data of our report (*1*). Each data set was permuted 99 times such that the observed character states of each character were shuffled randomly among taxa. The permuted data sets were searched for the most parsimonious tree under two constraints: (i) include and (ii) do not include billfishes plus butterfly mackerel as a monophyletic group. The length difference between trees never equalled or exceeded the length difference from the unpermuted *cytochrome b* data (*6*) (T-PTP = 0.01).
9. Briefly, degenerate primers were designed to the *lactate dehydrogenase b* locus with the use of amino acid alignments of all isozymes of LDH sequenced in vertebrates. a subset of the taxa examined in the *cytochrome b* study (*1*) were used in the second molecular study. The consensus aligned sequence for the scombroid fishes that were examined, after the insertion of alignment gaps, is 628 base pairs long (Finnerty and Block, unpublished results).
10. J. R. Finnerty and B. A. Block, *Fish. Bull. U.S.*, in press.
11. A. Knight and D. P. Mindell, *Syst. Biol.* **42**, 18 (1993).

18 January 1994; accepted 29 March 1994

Earthquake Aftershocks: Update

Since 1989, the U.S. Geological Survey has provided public forecasts of expected aftershock activity following major earthquakes in California, based on a stochastic model (*1*). The model represents the rate of aftershocks of magnitude M or larger as

$$\lambda(t, M) = 10^{a + b(M_m - M)}(t + c)^{-p}$$

where t is time after the mainshock, M_m is the mainshock magnitude, and a, b, p and c are constant parameters. Forecasts based on this model typically have been posed in probabilistic terms, such as, "There is a 50 percent chance of one or more magnitude 5 or larger earthquakes in the next 7 days." While such probabilistic statements may be clearly understood by scientists and emergency response officials, they often have created confusion and miscommunication among the press and general public. In an effort to more effectively communicate the aftershock hazard after the 17 January 1994

Northridge earthquake, we also provided the expected daily numbers of aftershocks of magnitude 3 and larger. We believe that this approach was better understood; it certainly reduced our need to explain some apparent paradoxes stemming from the public's unfamiliarity with statistical modeling. For example, it was frequently asked why our forecasts of probabilities of large aftershocks did not decrease after the occurrence of a large aftershock. The answer, which involves a discussion of the assumptions made in modeling aftershocks as a stochastic renewal process, is difficult to communicate in a press conference. The new forecasts of expected numbers of aftershocks more naturally conveyed a sense of how the Northridge aftershock sequence was decaying, and was expected to decay, with time. This approach, together with an explanation of the expected constant ratio in the numbers of large and small events, helped to communicate a sense of the temporal decay in earthquake hazard associated with large aftershocks.

The Northridge earthquake sequence was slightly more productive than the generic California sequence, given its mainshock magnitude of 6.7 (*2*). This characteristic was reflected in all our models. Estimates of the parameter *a* ranged from -1.1 ± 0.2 to -1.3 ± 0.2 during the first 10 days of the sequence, settling at -1.3, approximately 1 SD above the generic value -1.67. The decay rate and magnitude distribution parameters for the Northridge sequence ($p = 1.2$; $b = 0.9$) are both close to generic values of 1.08 and 0.91, respectively. To track the models' predictive success, we compared the model-predicted daily earthquake counts to the actual daily counts. Models obtained with the use of data from the first 1, 2, 5, and 10 days after the main shock were used to calculate the expected number of $M \geq 3$ aftershocks on each of the first 12 days of the sequence (Fig. 1). The actual counts of aftershocks in this period were generally well-predicted by those models based on data from two or more days. The model for the first 24 hours of the sequence overestimated *a*, underestimated *p*, and thus significantly overestimated the number of aftershocks in the days to follow. Such a lack of model constraint in the first 24 hours was expected on the basis of our earlier Monte Carlo experiments (*1*).

Table 1. Corrected version of table 1 in Reasenberg and Jones (*1*). Interval probabilities, $P(M_1, M_2, S,$ and $T)$, defined as the probability of one or more earthquakes occurring in the magnitude range ($M_1 \leq M < M_2$) and time range ($S \leq t < T$), for the generic California aftershock sequence. Top part gives probabilities for strong aftershocks or larger mainshocks ($M_1 = M_m - 1$, $M_2 = \infty$); bottom part gives probabilities for larger mainshocks only ($M_1 = M_m$, $M_2 = \infty$). Time intervals are described by *S* (interval start time, in days after the mainshock) and (*T*−*S*) (duration, in days). Model parameters for the generic sequence are ($b = 0.91$, $p = 1.08$, $a = -1.67$, and $c = 0.05$).

(*T*−*S*)	*S*								
	0.01	0.25	0.50	1	3	7	15	30	60
	Earthquakes with $M \geq M_m - 1$								
1	0.428	0.233	0.166	0.107	0.044	0.019	0.009	0.004	0.002
3	0.520	0.341	0.271	0.199	0.101	0.051	0.025	0.012	0.006
7	0.578	0.417	0.350	0.278	0.165	0.095	0.051	0.027	0.014
30	0.656	0.522	0.465	0.402	0.292	0.206	0.137	0.085	0.049
60	0.685	0.563	0.510	0.451	0.348	0.264	0.190	0.130	0.081
90	0.700	0.584	0.534	0.478	0.378	0.296	0.223	0.150	0.105
365	0.745	0.645	0.603	0.555	0.469	0.397	0.328	0.265	0.203
1000	0.770	0.681	0.643	0.599	0.522	0.456	0.394	0.335	0.275
	Earthquakes with $M \geq M_m$								
1	0.066	0.032	0.022	0.014	0.005	0.002	0.001	0.001	0.000
3	0.086	0.050	0.038	0.027	0.013	0.006	0.003	0.002	0.001
7	0.101	0.064	0.052	0.039	0.022	0.012	0.006	0.003	0.002
30	0.123	0.087	0.074	0.061	0.042	0.028	0.018	0.011	0.006
60	0.132	0.097	0.084	0.071	0.051	0.037	0.026	0.017	0.010
90	0.138	0.102	0.090	0.077	0.057	0.042	0.030	0.021	0.014
365	0.155	0.120	0.1-7	0.095	0.075	0.060	0.048	0.037	0.028
1000	0.165	0.131	0.119	0.106	0.087	0.072	0.060	0.049	0.039

Fig. 1. Northridge aftershock modeling. Observed numbers of ($M \geq 3.0$) aftershocks during the first 12 days of the Northridge earthquake sequence (diamonds) compared with expected daily counts of aftershocks predicted with statistical models. Models based on aftershock data for the first 1, 2, 5, and 10 days after the mainshock are shown with solid and broken lines. Corresponding numbers of aftershocks expected for generic sequences following magnitude 6.6, 6.8, and 7.0 mainshocks are shown for comparison.

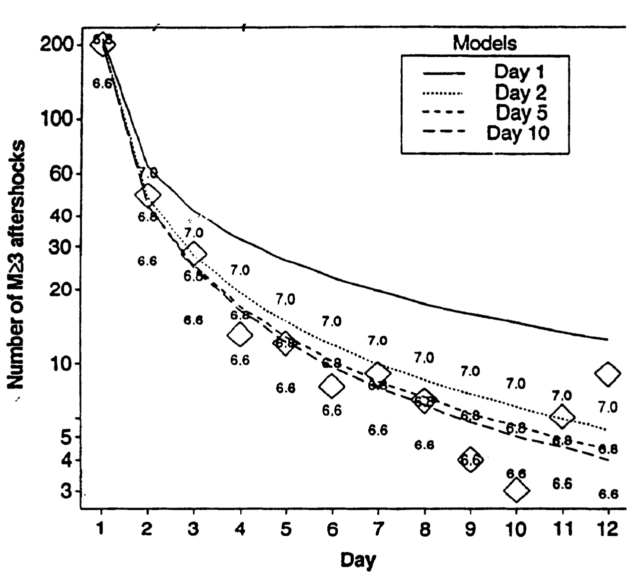

In the process of compiling modeling data (Fig. 1), we corrected an error in our formulation for calculating earthquake probabilities and expected numbers of aftershocks (*4*). The error arose from our incorrectly treating $\lambda(t, M)$ as a density function, when in fact it is a density with respect to *t* and a rate with respect to M. Thus, λ should not be integrated with respect to M to obtain the interval probabilities, as was indicated in equation 4 of our original report (*1*). This error, which entered into the calculation of tables 1 and 2 in our original report and in all estimates of aftershock probabilities to date (*3*), resulted in our underestimation of probabilities by up to a factor of approximately 2. However, the error did not affect the estimation of model parameters or the generic model in Reasenberg and Jones (*1*). Corrected probabilities for the generic California model, as defined in (*1*), have been calculated (Table 1).

P. A. Reasenberg
U.S. Geological Survey,
345 Middlefield Road,
Menlo Park, CA 94025, USA
L. M. Jones
U.S. Geological Survey,
525 South Wilson Boulevard,
Pasadena, CA 91106, USA

REFERENCES AND NOTES

1. P. A. Reasenberg and L. M. Jones, *Science* **243**, 1173 (1989).
2. The moment magnitude, M_w, is 6.7. The earthquake produced an aftershock sequence roughly comparable, in numbers and magnitudes of aftershocks, to a generic sequence after a $M_w = 6.8$ mainshock.
3. The modeling results presented here were obtained with the corrected versions of our programs.
4. We are grateful to J. C. Pechmann for pointing out the error. We apologize to our colleagues who have used the erroneous programs.

25 April 1994; accepted 28 April 1994